NASA

MEMORANDUM

FLUTTER TESTS OF SOME SIMPLE MODELS AT A

MACH NUMBER OF 7.2 IN HELIUM FLOW

By Homer G. Morgan and Robert W. Miller

Langley Research Center
Langley Field, Va.

NATIONAL AERONAUTICS AND SPACE ADMINISTRATION

WASHINGTON

April 1959

NATIONAL AERONAUTICS AND SPACE ADMINISTRATION

MEMORANDUM 4-8-59L

FLUTTER TESTS OF SOME SIMPLE MODELS AT A

MACH NUMBER OF 7.2 IN HELIUM FLOW*

By Homer G. Morgan and Robert W. Miller

SUMMARY

Results of hypersonic flutter tests on some simple models are pre-
sented. The models had rectangular plan forms of panel aspect ratio 1.0,
no sweepback, and bending-to-torsion frequency ratios of about 1/3. Two
airfoil sections were included in the tests; double wedges of 5-, 10-,
and 15-percent thickness and flat plates with straight, parallel sides
and beveled leading and trailing edges. The models were supported by a
cantilevered shaft.

The double-wedge wings were tested in helium at a Mach number of 7.2.
An effect of airfoil thickness on flutter speed was found, thicker wings
requiring more stiffness to avoid flutter. A few tests in air at a Mach
number of 6.9 showed the same thickness effect and also indicated that
tests in helium would predict conservative flutter boundaries in air.
The data in air and helium seemed to be correlated by piston-theory cal-
culations. Piston-theory calculations agreed well with experiment for
the thinner models but began to deviate as the thickness parameter $M\tau$
approached and exceeded 1.0.

A few tests on flat-plate models with various elastic-axis locations
were made. Piston-theory calculations would not satisfactorily predict
the flutter of these models, probably because of their blunt leading
edges.

Author

INTRODUCTION

Piston theory has been proposed by Lighthill (ref. 1) as a simple
method for calculating oscillatory aerodynamic forces at high Mach num-
bers. Various other authors (for example, refs. 2 to 4) have developed

---

*Title, Unclassified.

piston theory and applied it to trend studies of flutter characteristics. However, experimental data have not been available to determine the limits of applicability of this theory. Information which needs to be established includes the upper and lower Mach number bounds and the airfoil shapes and maximum airfoil thickness permitted by the theory. In addition, a predicted effect of airfoil thickness and shape on flutter speed has not been adequately demonstrated.

In the present investigation, an attempt was made to isolate some of the thickness and shape effects predicted by piston theory by using models with double-wedge airfoils of varying thickness and some beveled-edge flat-plate models. The double-wedge models also permitted a partial evaluation of a restriction on piston theory given in reference 1 - that w/a must be less than 1.0, where w is the downwash velocity and a is the free-stream speed of sound. For double-wedge models, this restriction reduces to $U\tau/a = M\tau < 1.0$ where U is the free-stream velocity, τ is the thickness ratio and M is the Mach number. In order to assess these aerodynamic effects, the models chosen for the investigation were very simple to allow the structural portion of the flutter problem to be treated without difficulty. Also, the bending-to-torsion frequency ratio was kept low $(\omega_h/\omega_\alpha \approx 1/3)$ since trend studies (ref. 4) indicate that the largest effects of airfoil shape and thickness are in this range.

The present investigation utilized helium as a testing medium to obtain flutter data at a Mach number of 7.2. Wind tunnels utilizing helium have previously been used extensively for studying hypersonic-flow phenomena. (See, for example, refs. 5 and 6.) These studies, however, have been conducted to examine steady flow problems such as total loads or local pressure distributions. Meanwhile, very little flutter data exist at hypersonic speeds. Most of the available information is given in references 7 and 8 and was obtained at a Mach number of 6.9 in air.

Helium has two primary advantages as a hypersonic test medium when compared with air: (1) Higher Mach numbers can be obtained without requiring the addition of heat to a system since helium has a much lower liquefying temperature than air. (2) Higher dynamic pressures can be obtained at the same Mach number and stagnation pressure because helium has a larger ratio of specific heats than air. Thus, use of helium results in a less complicated and less expensive wind-tunnel facility to produce the same test conditions. The higher dynamic pressures available in helium as compared with air at the same storage pressure and the feasibility of using atmospheric stagnation temperatures with helium are especially attractive for flutter testing since model design and construction are greatly simplified.

A few test runs were made in air at a Mach number of 6.9 in an attempt to correlate data on flutter models tested in two mediums.

SYMBOLS

a   free-stream speed of sound, ft/sec

b   semichord, in.

C_p pressure coefficient

c   chord, in.

d   shaft width, in.

f   frequency, cps

I_α mass moment of inertia about the elastic axis per unit length, slug-ft^2/ft

M   Mach number

m   mass per unit length, slugs/ft

p_o stagnation pressure, lb/sq ft

q   dynamic pressure, lb/sq ft

R $\dfrac{b\omega_\alpha}{a}\sqrt{\mu}$, a stiffness-altitude parameter

S_α static unbalance about the elastic axis per unit length, positive for center of gravity back of elastic axis, slug-ft/ft

t   shaft thickness, in.

U   free-stream velocity, ft/sec

w   downwash velocity, ft/sec

x_o elastic-axis position in fraction of the chord, measured from the leading edge
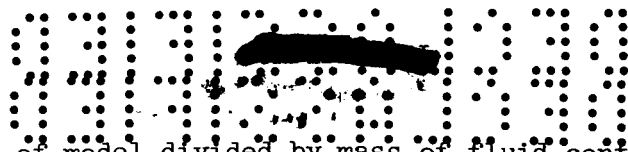
μ mass of model divided by mass of fluid contained in a cylinder determined by the model, $m/\pi\rho b^2$

ρ density of test medium, slugs/cu ft

τ maximum thickness of model in fraction of the chord

ω circular frequency, radians/sec

Subscripts:

c   calculated quantity

e   experimentally determined quantity

f   quantity at flutter

h   bending mode

α torsion mode

∞ free-stream conditions

APPARATUS

Langley Hypersonic Aeroelasticity Tunnel

Most of the tests were performed in the Langley hypersonic aeroelasticity tunnel which uses helium as a test medium. A sketch of this blowdown tunnel is shown in figure 1. The nozzle used in the tests has circular cross sections with a 1.41-inch-diameter minimum section and an 8-inch-diameter test section. Helium is supplied to the stagnation chamber at pressures up to 1,200 pounds per square inch from which dynamic pressures of over 5,000 pounds per square foot are obtainable. The downstream end of the tunnel is connected to a vacuum chamber which can be operated at pressures as low as 1/2 inch of mercury absolute. Stagnation temperature is essentially constant during a run and corresponds to atmospheric temperature. With the available high-pressure helium supply, test runs are of approximately 30-second duration.

Models are wall-mounted on a removable plate which is contoured to maintain a circular test section. The opposite wall is made of transparent plastic; thus, the model could be observed during the test runs. Mach number surveys have been made across the diameter of the tunnel at
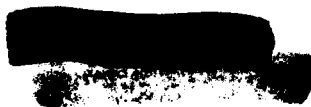
the center of the test section and 4 inches upstream and $1\frac{1}{8}$ inches down-
stream from the center of the test section. The results are shown in
figure 2. The Mach number at the center of the test section, where the
models are located, is about 7.2 and remains practically constant over
the span of the model.

Langley 11-Inch Hypersonic Tunnel

Three test runs were made in the Langley 11-inch hypersonic tunnel
which produces a Mach number of 6.9 when air is used as a test medium.
The characteristics of this tunnel are given in reference 9.

MODELS

Configuration

All models tested had panel aspect ratios of 1.0, no taper, zero
sweep, and 4-inch span. The models were supported by a shaft which was
2 inches long. The shaft was cantilevered at the tunnel wall; thus, the
model was held outside the boundary layer and in a region of uniform
flow. Strain gages for determining model response were attached to the
shaft. The shaft was covered by a fairing which was rigidly attached to
the tunnel wall. Provision was made for a clamping device which extended
from the tunnel wall along the leading edge of the fairing and restrained
the model during the starting transient. However, this device was found
to be unnecessary and its use was discontinued after the first few tests.
A photograph of a typical model, ready for installation in the test sec-
tion, is shown in figure 3.

Construction

Details of the model construction are shown in figures 4(a) and 4(b).
Two types of models were tested: models 1 to 4 were flat plates with
beveled leading and trailing edges (fig. 4(a)) whereas models 5 to 17
were double-wedge airfoils (fig. 4(b)).

The flat-plate models were solid aluminum alloy with an integral
shaft. The center line of the shaft was varied along the chord of the
wing to change the elastic-axis position. The leading and trailing edges
were beveled at a 45° angle.

The double-wedge models had a steel core which was integral with the
shaft. Balsa, which formed the airfoil contour, was glued to the core
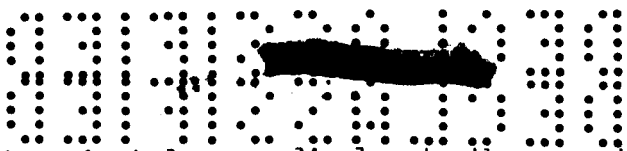
with its grain oriented perpendicular to the core to minimize the stiffness contribution of the wood. Part of the core was drilled out, before covering with balsa, to reduce the model weight. Models of 5-, 10-, and 15-percent thickness were tested. The elastic axis of this group of models was at 45 percent chord.

Physical Parameters

The mass parameters of the models are listed in table I along with pertinent dimensions. These data were measured prior to installing the models in the tunnel. The mass of the shaft is not included in the data shown.

All models were vibrated with an acoustic shaker before testing and the vibration nodes and frequencies were determined. Typical nodal patterns for both types of models are shown in figure 5. In all cases examined, the third and fourth frequencies, corresponding to second bending and second torsion, were well above the first and second frequencies. $\left(\text{As an example, model 10 had frequencies of } f_{h_1} = 20.5 \text{ cps,}\right.$ $f_{\alpha_1} = 64.5 \text{ cps,} \quad f_{h_2} = 188 \text{ cps, and} \quad f_{\alpha_2} = 402 \text{ cps.}\Big)$ Since the flutter frequency always fell between first bending and first torsion, the third and fourth frequencies were not determined for all cases. The natural frequencies are listed in table I.

TEST PROCEDURE

Models were mounted in the test section at zero angle of attack. Then, after installation in the tunnel and just prior to the test run, the first two natural frequencies of the model were checked.

For the flutter tests, flow was established in the tunnel at a low dynamic pressure. Then, with the Mach number remaining constant, dynamic pressure was increased until the model fluttered or maximum operating conditions were reached. Stagnation temperature and pressure and signals from the strain gages mounted on the model shafts were recorded on an oscillograph throughout the test. Conditions at flutter were established by correlating the stagnation quantities recorded on the oscillograph record with the model response given by the strain-gage signals.

ANALYSIS

Flutter calculations were made on the models by using two uncoupled modes. The modes used were chosen after examination of photographs of the modes for similar models. These photographs indicated that it would be reasonable to assume that the torsion mode consisted of unit twist along the entire span and the bending mode was the straight line given by

$$F_h = 1/4(1 + 3\eta)$$

(F_h is the displacement at the elastic axis and η is a spanwise variable which is zero at the root and unity at the tip.) The calculated flutter results were found to be relatively insensitive to the slope of this line. The frequencies associated with these modes were those which were measured and are listed in table I.

The distributed mass properties used in the calculations were those listed in table I. The mass of the shaft is not included in these calculations.

The aerodynamic forces were obtained from second-order piston theory. The coefficients are presented in reference 2. Airfoil-shape terms were included for the flat-plate models as well as for the double-wedge models.

RESULTS AND DISCUSSION

The results of the tests are listed in table II. The test medium, frequency ratios, and test-section conditions are shown at flutter. For tests where no flutter occurred, the conditions which are given correspond to the maximum dynamic pressure reached during the test. A stiffness-altitude parameter $R = \dfrac{b\omega_\alpha}{a}\sqrt{\mu}$ is also shown at flutter or at the maximum dynamic pressure. This parameter has been shown by piston theory calculations to be useful for correlating flutter data at high Mach numbers for the range of density ratios covered by the investigation.

The stiffness-altitude parameter depends only upon the physical properties of the wing - in particular, the torsional stiffness - and upon the atmosphere in which it operates. Its value increases as either
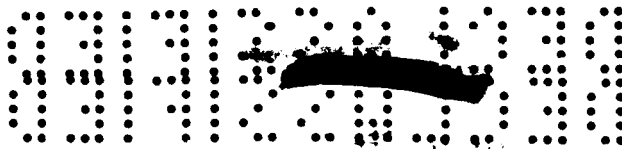
the altitude or the stiffness increase. The stable region, when this parameter is the ordinate, will be above the flutter boundary.

Double-Wedge Models

Experiment.- The experimental results from table II for the double-wedge models are plotted in figure 6 as functions of the thickness parameter M_T. As mentioned earlier, the parameter M_T has certain significance concerning the limits of piston-theory applicability. The ratio of flutter frequency to torsion frequency is shown in figure 6(a). This frequency ratio exhibits considerable scatter at any particular value of M_T but is relatively constant with thickness (or M_T). The flutter frequency varies from 45 percent to 65 percent of the torsional frequency, whereas the bending frequency is about one-third the torsional frequency.

Examination of the stiffness-altitude parameter for the double wedges (fig. 6(b)) reveals a definite thickness effect. As M_T increases, the value of the stiffness-altitude parameter increases; thus, flutter occurred at a higher altitude or with greater stiffness. Although considerable scatter is evident from the data, the general trend is for the thickness effect to be nonlinear with thickness and to decrease as M_T increases.

Also shown in figure 6 are data obtained both in air (at $M = 6.9$) and in helium (at $M = 7.2$). Only three runs were made in air; the 10- and 15-percent-thick models fluttered and the 5-percent-thick model would not flutter at the available dynamic pressure. The flutter frequency, obtained from the models which did flutter, is seen from figure 6(a) to correlate very well with flutter frequencies determined in helium. From figure 6(b), the stiffness-altitude parameter at flutter is seen to be 20 to 25 percent lower in air than in helium on the two models which fluttered. This result would indicate that studies made in helium at this Mach number would predict flutter boundaries which would be conservative in air. However, as will be pointed out later, these differences may be accounted for by using piston-theory calculations.

Calculations.- The thickness effects predicted by piston theory, which is used to determine aerodynamic forces in these calculations, change drastically with frequency ratio. The models in the test program were designed to have bending-to-torsion frequency ratios of approximately one-third, in the range where the predicted effects are large. A comparison between calculations and experiment on models 5, 6, and 7 is shown in figure 7 to illustrate this variation with frequency ratio. Figure 7 shows that the calculations agree very well
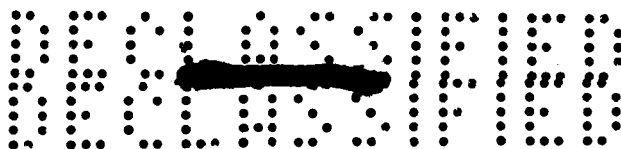
with experiment on the 5- and 10-percent-thick models which were tested at $M = 7.2$ in helium. Calculations on the 15-percent-thick wing predict a greater effect of thickness than is measured. As the frequency ratio approaches 1.0, the calculations show flutter at much higher altitudes, although the magnitude of the thickness effect is much reduced.

A summary of flutter calculations on all the double-wedge wings plotted against the thickness parameter $M\tau$ is shown in figure 8. The ratio of experimentally determined flutter frequency to calculated flutter frequency is given in figure 8(a). In all cases, calculated flutter frequencies are too high. However, air and helium data all fall within the same scatter band.

The ratio of experimental stiffness-altitude parameter to calculated stiffness-altitude parameter is plotted in figure 8(b). The trend is for the calculations to give poorer agreement with experiment as the thickness parameter $M\tau$ becomes larger; thus piston theory is giving a poorer description of the aerodynamic forces. At $M\tau = 0.36$, calculations are within 8 percent of experiment; at $M\tau \approx 0.70$, calculations are all within 16 percent of experiment; and at $M\tau \approx 1.05$, calculations are all within 25 percent of experiment. A check calculation on some models using third-order piston theory actually showed poorer agreement with experiment than the calculations with second-order piston theory.

As shown in figure 8(b), flutter points obtained in air are calculated with about the same degree of accuracy as those obtained in helium. Calculations in air also show that the increase in stiffness-altitude parameter when the Mach number is changed from 6.9 to 7.2 is only about 4 percent. This difference is not as great as the experimental difference between air and helium shown in figure 6(b). However, the calculations in figure 8(b), which contain the variation in γ, the ratio of specific heats, do tend to correlate the data and suggest that piston-theory calculations may be used to extrapolate flutter data obtained in helium to air. The flutter calculations are affected by a change in the ratio of specific heats since this factor γ appears in the second term of the second-order piston-theory pressure coefficient

$$c_p = \frac{2}{M}\left(\frac{w}{U}\right) + \left(\frac{\gamma + 1}{2}\right)\left(\frac{w}{U}\right)^2$$

The thickness effect arises from the second term of this relation and, since γ is 1.67 for helium compared with 1.4 for air, flutter calculations in helium will show a larger thickness effect than flutter calculations in air.
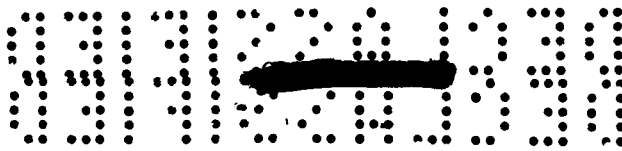
As mentioned previously, a restriction on the use of piston theory, as given in reference 1, is that w/a must be less than 1.0. If the downwash due to unsteady motion is neglected, this requirement for double-wedge airfoils becomes $M_T < 1.0$. (This condition is reasonable since flutter calculations are made for small perturbations at the neutral stability point.) This limitation on piston theory seems to be borne out at $M = 7.2$ by the comparison shown in figure 8.

Flat-Plate Models

Experiment.- The experimental results for the flat-plate models are shown in figure 9 where the stiffness-altitude parameter is plotted as a function of elastic-axis location in fraction of the chord. Figure 9(a) shows that the flutter frequencies are all less than 40 percent of the torsion frequency. Thus, flutter frequencies were about the same as the bending frequencies, which were approximately one-third of the torsion frequencies. By observation, the flutter mode was determined to be almost pure bending with only slight torsion components.

The stiffness-altitude parameter at flutter is plotted in figure 9(b). The no-flutter point was found on a model (number 1) whose frequencies were about 65 percent higher than those of the model with the same elastic-axis location which did flutter at a lower dynamic pressure (model number 2). The difference in the stiffness-altitude parameters possibly is explained by noting that the center of gravity of the model which fluttered is slightly farther back of the elastic axis whereas its radius of gyration is slightly less than the model which did not flutter.

Calculations.- A comparison of experiment and piston-theory calculations plotted against elastic-axis location is shown in figure 10. The ratio of experimental to calculated flutter frequencies is presented in figure 10(a). The experimental flutter frequencies are approximately one-half the calculated flutter frequencies. In figure 10(b), the ratio of experimental to calculated stiffness-altitude parameter is shown. Poor agreement of experiment and calculations is apparent for forward-axis locations, the calculated value being only 52 percent of the experimental value at $x_0 = 0.388$. The agreement improves as the axis moves rearward until the calculated value is about 95 percent of the experimental value at $x_0 = 0.513$.

These flat-plate models have airfoil sections which are straight-sided with a bevel at both the leading and trailing edges, as shown in figure 4. The bevel amounts to only $1\frac{1}{4}$ percent of the chord at each end of the model. This bevel appears to be such a small fraction of

the chord that the airfoil would be expected to behave like a zero-thickness plate. (For flat sides, the slope of the airfoil contour is zero and second-order piston theory will not give a thickness effect.) However, all calculations made on these models by assuming zero thickness gave infinite flutter speeds. The calculations presented in figure 10 use the piston-theory thickness term, which includes the effect of the bevels at the edges, despite the fact that the requirement for $w/a < 1.0$ is violated in the region of the bevel. Using this term apparently overestimates the shape effect, at least for forward-axis locations.

A possibility for explaining the poor agreement of experiment and calculations is the inability of the theory to account for a blunt leading edge. Studies of blunt-nosed slender bodies (for example, ref. 10) have revealed a pressure carryover along the forward portion of the body due to the blunt leading edge and its detached shock wave. Since flutter of an aerodynamic surface is known to be very sensitive to the relative position of the center of pressure and elastic axis, such a pressure carryover on an oscillating airfoil could well have large effects on the flutter characteristics.

<center>CONCLUDING REMARKS</center>

Tests at a Mach number of 7.2 in helium on simple models having double-wedge airfoils of various thicknesses indicate a large effect of thickness on flutter speed. As airfoil thickness increases, the models require more stiffness at a given altitude to avoid flutter. The thickness effect on flutter speed is nonlinear, its magnitude decreasing with increasing airfoil thickness.

A limited number of tests on similar models at a Mach number of 6.9 in air indicate the same trends with thickness as were observed in helium tests. Comparison of tests in air and helium indicates that flutter boundaries obtained in helium would be conservative in air, possibly because of the differences in the ratios of specific heat.

Piston-theory calculations on the double-wedge models agree fairly well with experiment for the thinner airfoils. As the thickness increases, such that the thickness parameter $M\tau$ approaches and exceeds one, agreement between the calculations and experiment becomes poorer. Tests in air and helium were calculated with about the same accuracy and are correlated by the piston-theory calculations; thus tests in helium can be extrapolated to air conditions with some confidence.

The flutter of some flat-plate models having beveled edges could not be calculated with reasonable accuracy by using the piston theory. The

failure of piston theory to calculate flutter on these models can probably be attributed to the effect of the very blunt leading edges of the model.

Langley Research Center,
     National Aeronautics and Space Administration,
          Langley Field, Va., January 9, 1959.

REFERENCES

1. Lighthill, M. J.: Oscillating Airfoils at High Mach Number. Jour. Aero. Sci., vol. 20, no. 6, June 1953, pp. 402-406.

2. Ashley, Holt, and Zartarian, Garabed: Piston Theory - A New Aerodynamic Tool for the Aeroelastician. Jour. Aero. Sci., vol. 23, no. 12, Dec. 1956, pp. 1109-1118.

3. Chawla, Jagannath P.: Aeroelastic Instability at High Mach Number. Jour. Aero. Sci., vol. 25, no. 4, Apr. 1958, pp. 246-258.

4. Morgan, Homer G., Runyan, Harry L., and Huckel, Vera: Theoretical Considerations of Flutter at High Mach Numbers. Jour. Aero. Sci., vol. 25, no. 6, June 1958, pp. 371-381.

5. Hammitt, A. G., and Bogdonoff, S. M.: A Study of the Flow About Simple Bodies at Mach Numbers From 11 to 15. WADC Tech. Rep. 54-257, Wright Air Dev. Center, U. S. Air Force, Oct. 1954.

6. Erickson, Wayne D.: Study of Pressure Distributions on Simple Sharp-Nosed Models at Mach Numbers From 16 to 18 in Helium Flow. NACA TN 4113, 1957.

7. Runyan, Harry L., and Morgan, Homer G.: Flutter at Very High Speeds. NACA RM L57D16a, 1957.

8. Lauten, William T., Jr., Levey, Gilbert M., and Armstrong, William O.: Investigation of an All-Movable Control Surface at a Mach Number of 6.86 for Possible Flutter. NACA RM L58B27, 1958.

9. McLellan, Charles H., Williams, Thomas W., and Beckwith, Ivan E.: Investigation of the Flow Through a Single-Stage Two-Dimensional Nozzle in the Langley 11-Inch Hypersonic Tunnel. NACA TN 2223, 1950.

10. Lees, Lester, and Kubota, Toshi: Inviscid Hypersonic Flow Over Blunt-Nosed Slender Bodies. Jour. Aero. Sci., vol. 24, no. 3, Mar. 1957, pp. 195-202.

TABLE I.- MODEL PARAMETERS

Model	d, in.	t, in.	τ	x_o	m, slugs/ft	S_α, slug-ft/ft	I_α, slug-ft²/ft	f_{h_1}, cps	f_{α_1}, cps	f_{h_2}, cps	f_{α_2}, cps	$\dfrac{a_{h_1}}{a_{t_1}}$
						Flat-plate airfoil section						
1	0.75	0.091	0.023	0.450	1.36×10^{-2}	0.21×10^{-3}	1.31×10^{-4}	41.1	123	342	---	0.33
2	.25	.100	.025	.450	1.47	.25	1.38	24.5	73.5	---	---	.33
3	.25	.100	.025	.513	1.49	-.06	1.28	24.8	73.5	289	835	.34
4	.25	.100	.025	.388	1.48	.53	1.43	25.4	76.2	296	830	.33
						Double-wedge airfoil section						
5	0.75	0.036	0.05	0.450	0.89×10^{-2}	0.11×10^{-3}	0.90×10^{-4}	19.1	58.2	144	273	0.33
6	.75	.036	.10	.450	1.25	.25	1.29	17.8	56.0	158	---	.32
7	.75	.036	.15	.450	1.19	.21	1.32	18.4	58.3	176	244	.32
8	.75	.065	.05	.450	1.49	.19	1.20	32.7	104	220	440	.31
9	.50	.065	.05	.450	1.51	.22	1.36	28.1	92.0	---	---	.31
10	.25	.065	.05	.450	1.51	.22	1.36	20.5	64.5	188	402	.32
11	.25	.065	.10	.450	1.63	.20	1.69	19.6	58.0	---	---	.34
12	.25	.065	.15	.450	1.75	.34	1.93	18.3	54.0	196	442	.34
13	.75	.036	.05	.450	1.01	.16	1.04	19	59	144	280	.32
14	.75	.036	.10	.450	1.12	.17	1.25	19	56	161	---	.34
15	.75	.036	.15	.450	1.21	.17	1.29	18	58	---	---	.31
16	.25	.065	.10	.450	1.63	.28	1.72	19.8	59.2	---	---	.33
17	.25	.065	.15	.450	1.78	.32	1.94	17.6	52.0	---	---	.34

TABLE II.- COMPILATION OF TEST RESULTS

Model	Test medium	M	M_T	q, lb/sq ft	ρ, slugs/cu ft	a, ft/sec	μ	R_e	R_c	$\left(\dfrac{\omega_r}{\omega_\alpha}\right)_e$	$\left(\dfrac{\omega_r}{\omega_\alpha}\right)_c$	Remarks
1	Helium	7.2	0.16	2,678	0.0001700	780	917	5.00	3.70		0.75	No flutter
2	Helium	7.2	.18	739	.0000446	799	3,773	5.92	3.81	0.39	.74	
3	Helium	7.2	.18	1,032	.0000616	804	2,773	5.04	4.47	.33	.70	
4	Helium	7.2	.18	1,063	.0000638	802	2,658	5.13	2.77	.36	.76	
5	Helium	7.2	.36	722	.0000463	775	2,202	3.69	3.54	.51	.76	
6	Helium	7.2	.72	489	.0000291	805	4,918	5.11	5.14	.56	.74	
7	Helium	7.2	1.08	442	.0000247	830	5,510	5.45	6.01	.46	.75	
8	Helium	7.2	.36	2,240	.0001432	777	1,192	4.84				No flutter
9	Helium	7.2	.36	2,025	.0001285	780	1,346	4.53				No flutter
10	Helium	7.2	.36	1,260	.0000812	774	2,132	4.03	3.73	.65	.73	
11	Helium	7.2	.72	901	.0000533	807	3,506	4.45	5.15	.51	.76	
12	Helium	7.2	1.08	589	.0000363	791	5,526	5.31	6.12	.61	.75	
13	Air	6.9	.35	694	.0001336	467	973	4.12	3.88		.75	No flutter
14	Air	6.9	.69	650	.0001247	469	1,030	4.01	4.59	.57	.77	
15	Air	6.9	1.04	599	.0001041	492	1,326	4.50	5.63	.49	.76	
16	Helium	7.2	.72	752	.0000396	856	4,713	4.97	5.13	.61	.75	
17	Helium	7.2	1.08	570	.0000295	863	6,905	5.23	6.17	.48	.75	
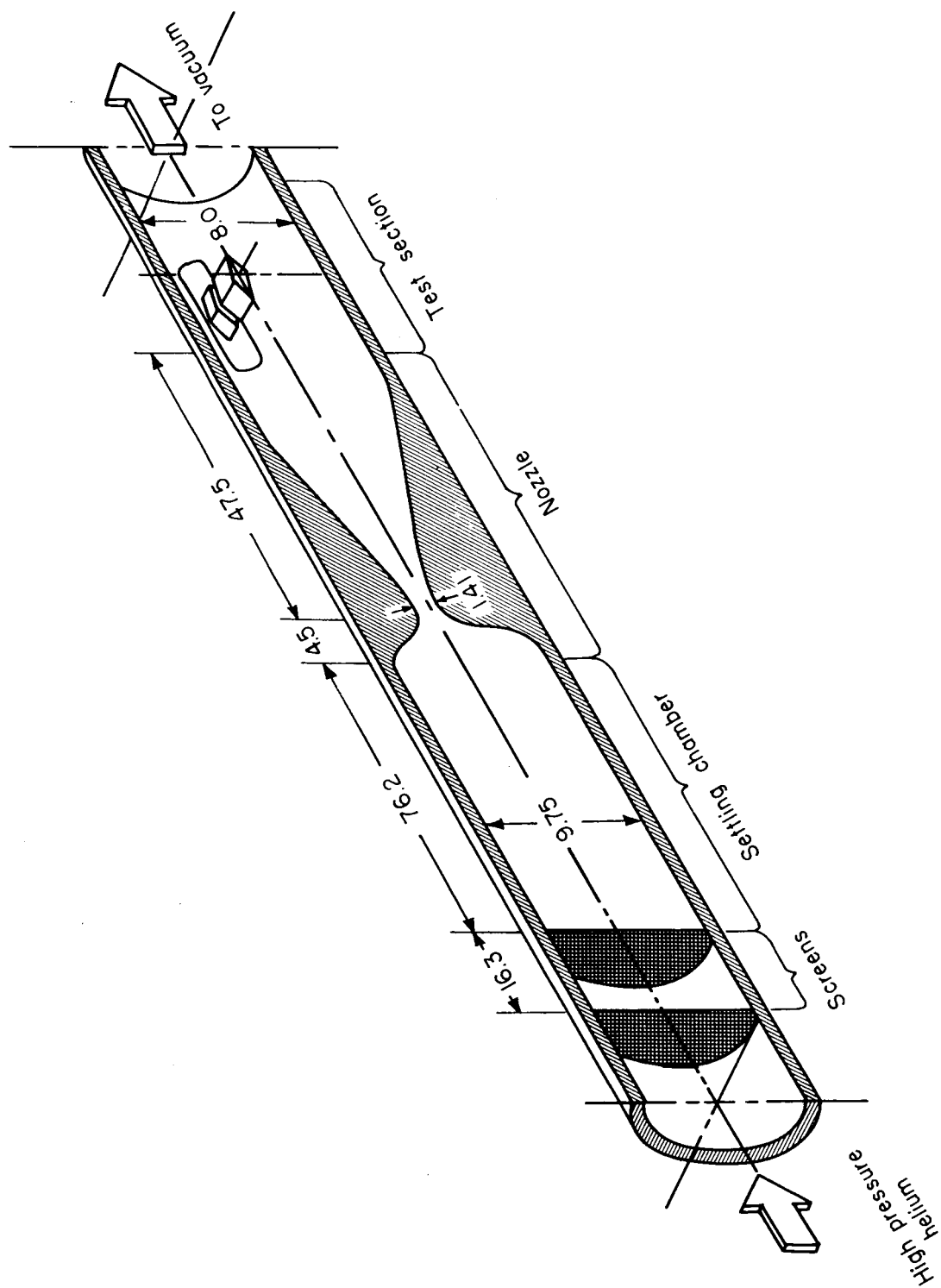
Figure 1.- Sketch of the Langley hypersonic aeroelasticity tunnel with a wall-mounted flutter model. All dimensions are in inches.

3U
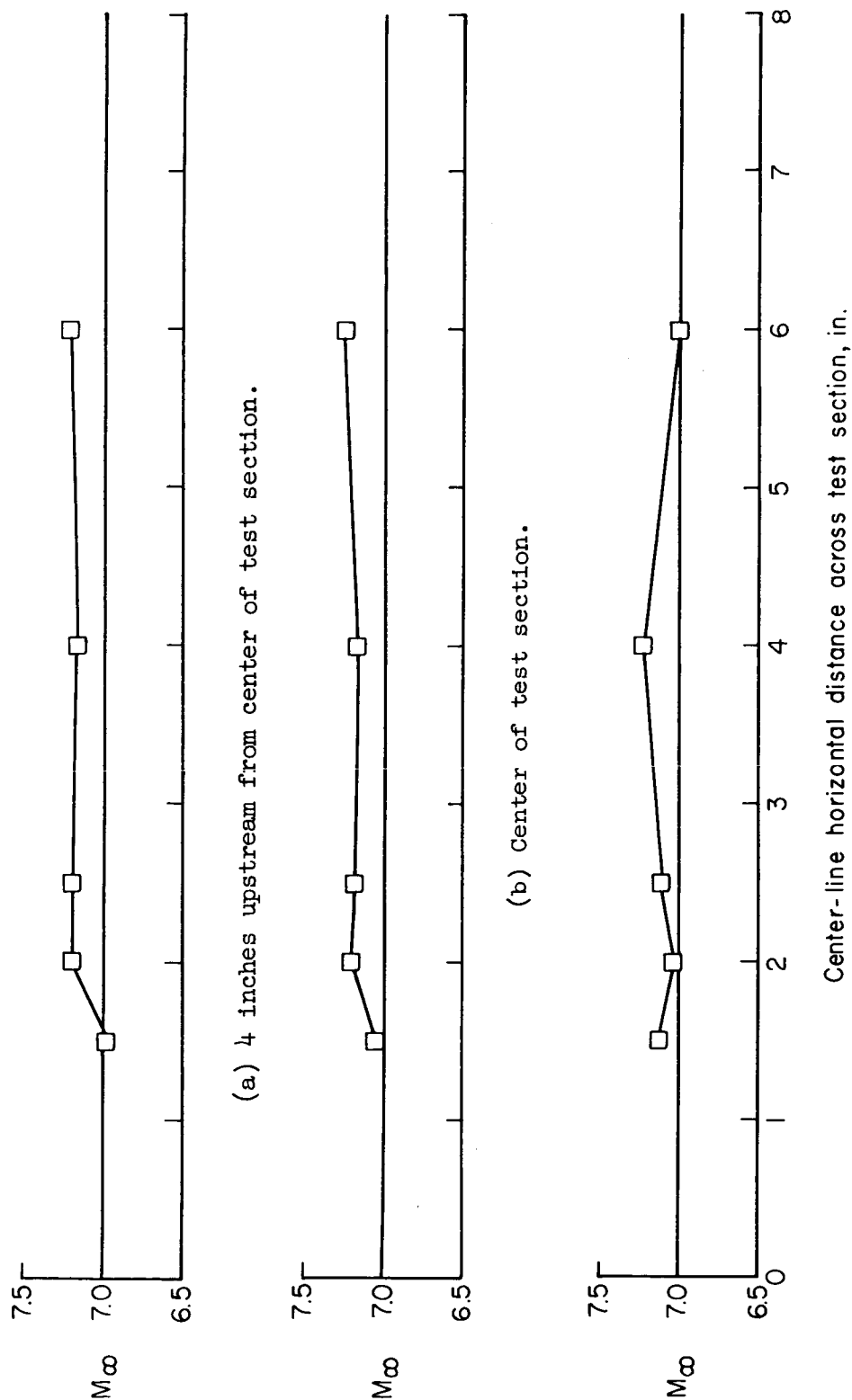
L-199

(a) 4 inches upstream from center of test section.

(b) Center of test section.

(c) $1\frac{1}{8}$ inches downstream from center of test section.

Center-line horizontal distance across test section, in.

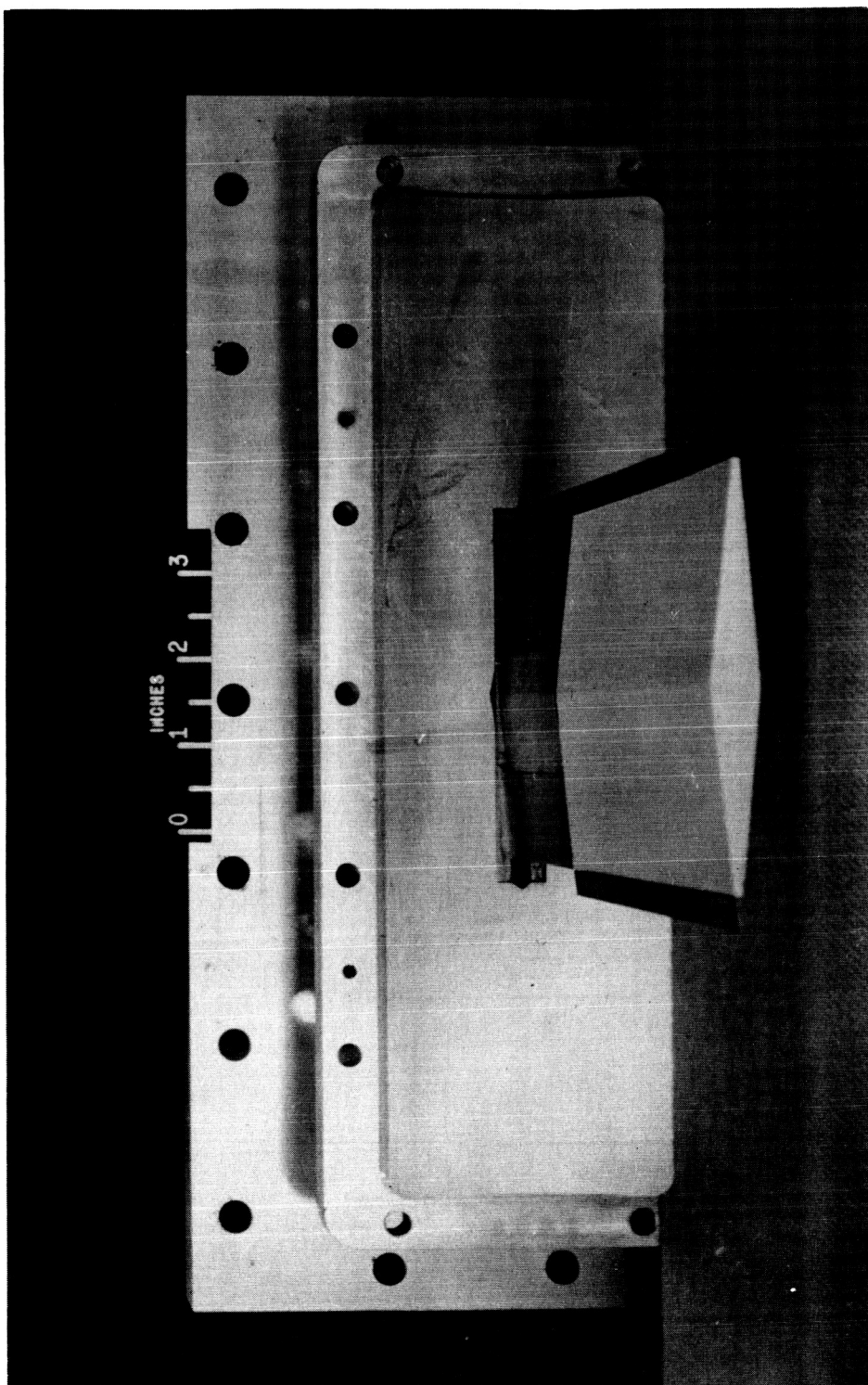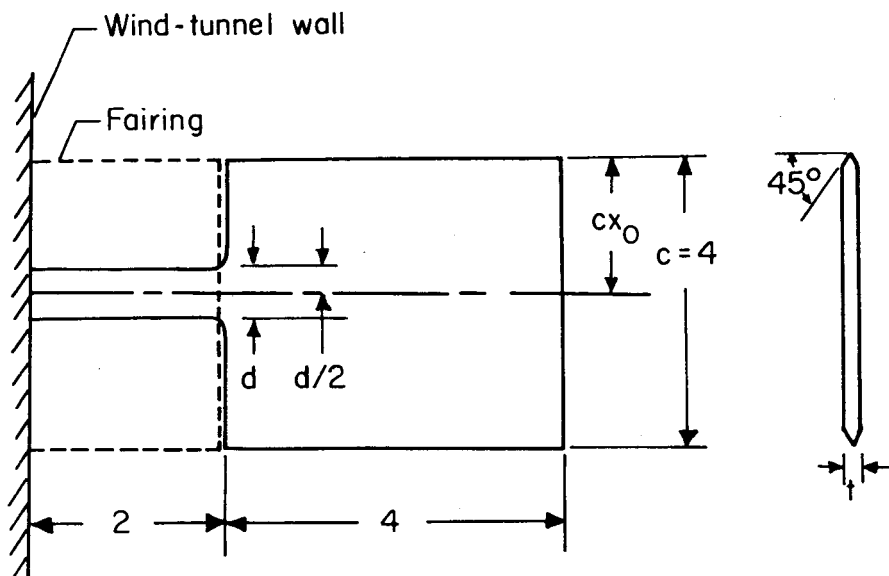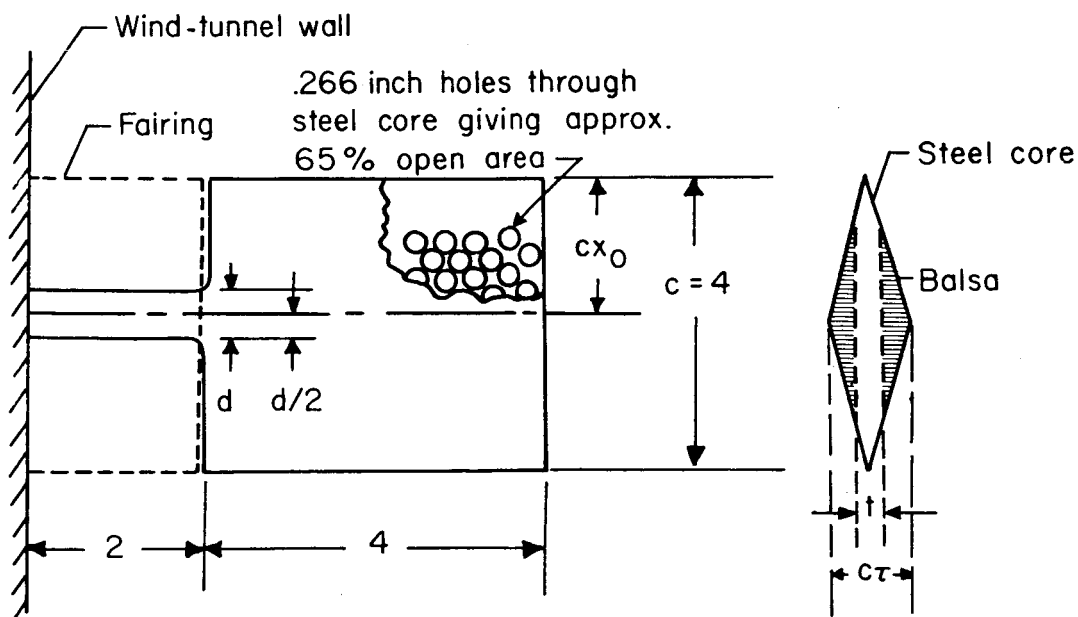Figure 2.- Mach number distribution across the test section of the Langley hypersonic aeroelasticity tunnel. $p_0 = 500$ lb/in².

Figure 3.- Photograph of a typical model ready for installation in the Langley hypersonic aeroelasticity tunnel.

L-58-3035

L-199

Wind-tunnel wall

Fairing

cx_0

$c = 4$

d $d/2$

2   4

45°

t

(a) Aluminum-alloy flat-plate models.

Wind-tunnel wall

Fairing

.266 inch holes through
steel core giving approx.
65% open area

cx_0

$c = 4$

d $d/2$

2   4

Steel core

Balsa

t

$c\tau$

(b) Double-wedge models.

Figure 4.- Sketch of the flutter models.   Dimensions are in inches.

— — · — — Second mode

— — · · — Third mode

— — — — — Fourth mode
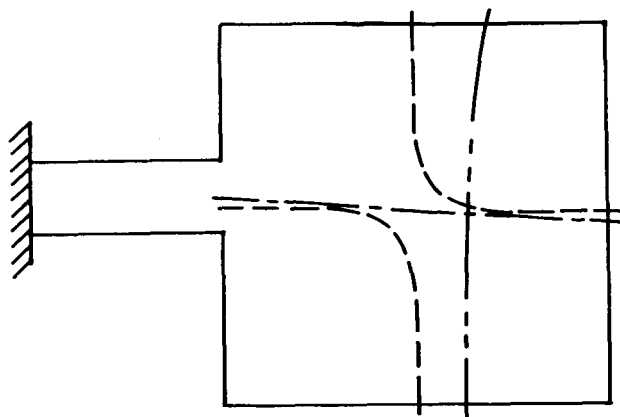
(a) Flat-plate models.
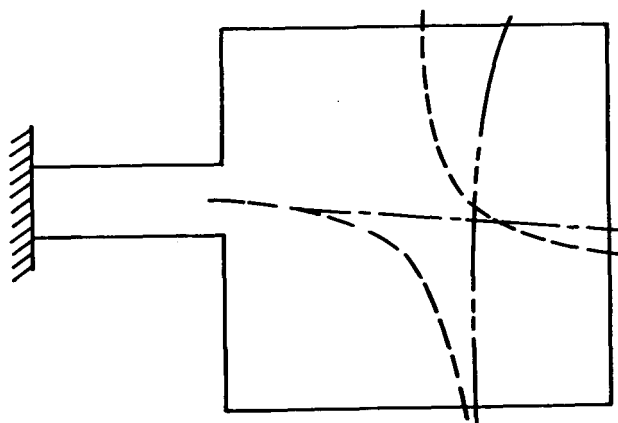
(b) Double-wedge models.

Figure 5.- Typical nodal patterns for the first four vibration modes of the test specimens.
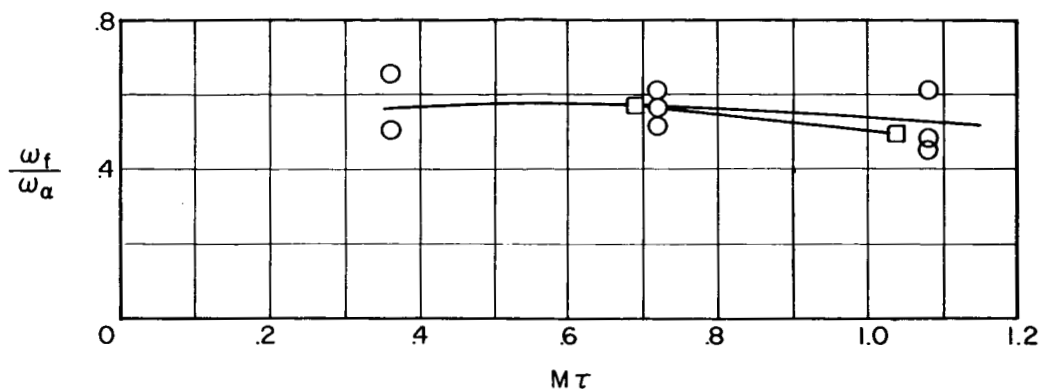
(a) Ratio of flutter frequency to torsional frequency.
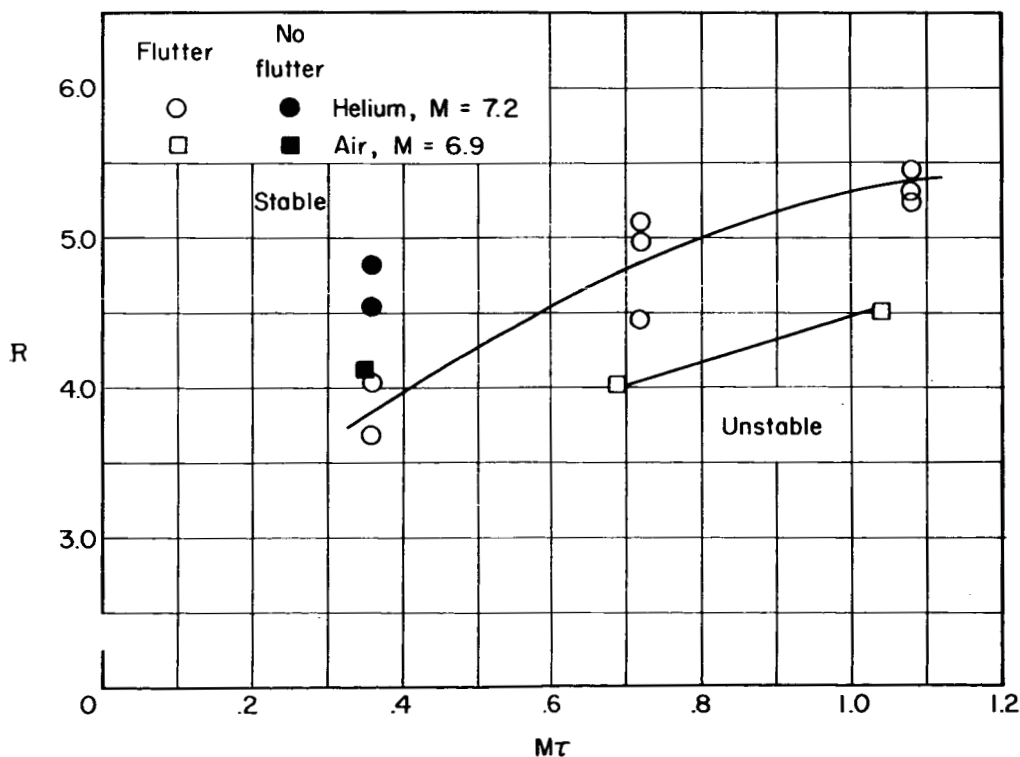
(b) Stiffness-altitude parameter.

Figure 6.- Experimental flutter results on double-wedge models plotted against the thickness parameter $M\tau$. $0.31 \leqq \omega_h/\omega_\alpha \leqq 0.34$; $x_o = 0.45$;

$$R = \frac{b\omega_\alpha}{a} \sqrt{\mu}.$$
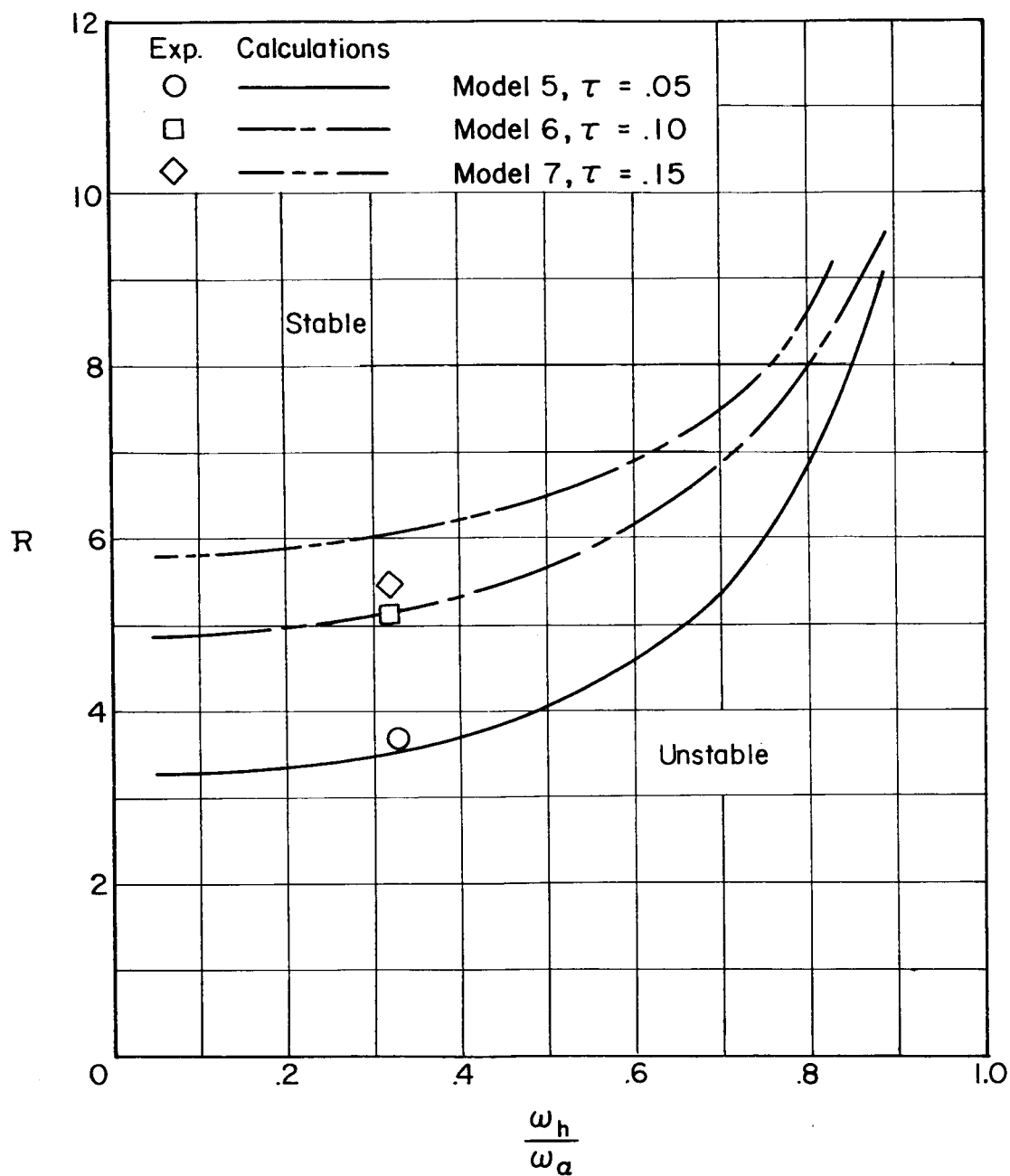
Figure 7.- Stiffness-altitude parameter at flutter plotted against frequency ratio for double-wedge models tested in helium at $M = 7.2$. $x_0 = 0.45$; $R = \frac{b\omega_\alpha}{a}\sqrt{\mu}$.

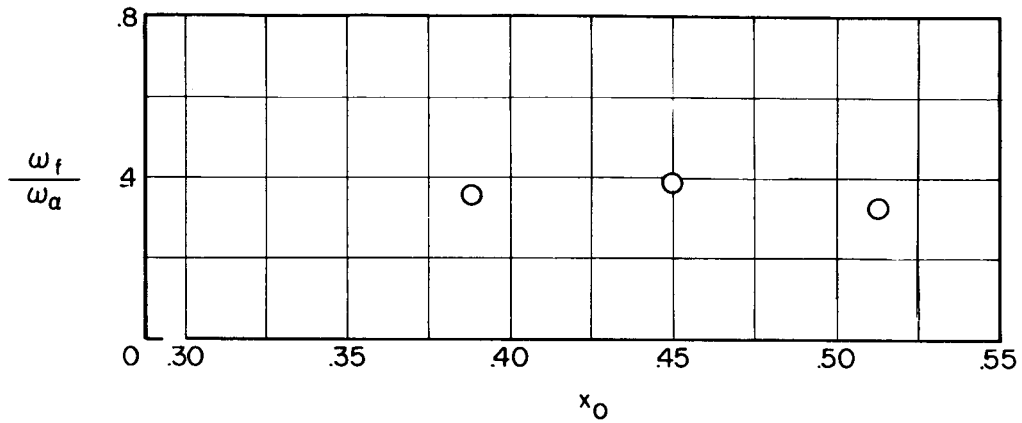(a) Ratio of experimental flutter frequency to calculated flutter frequency.
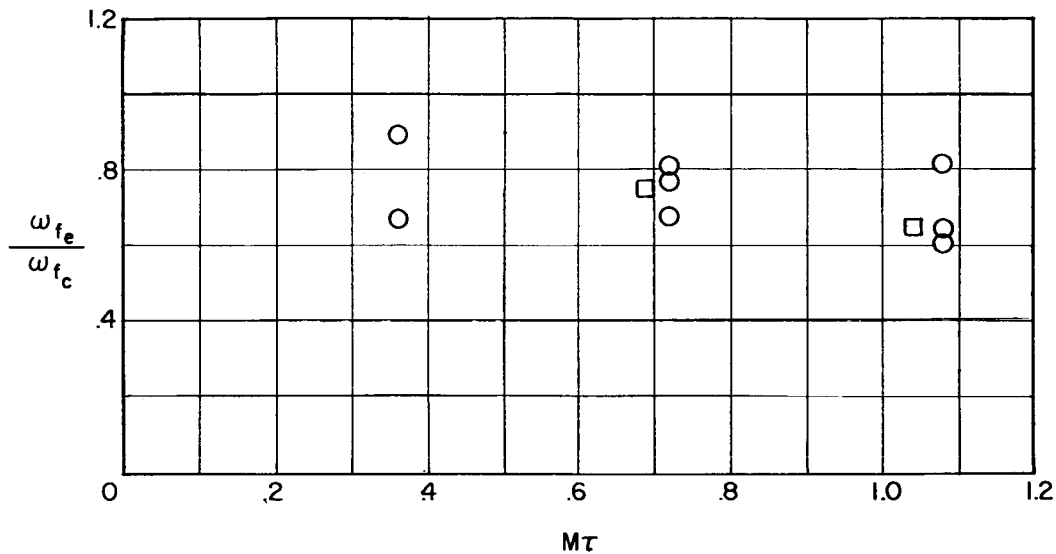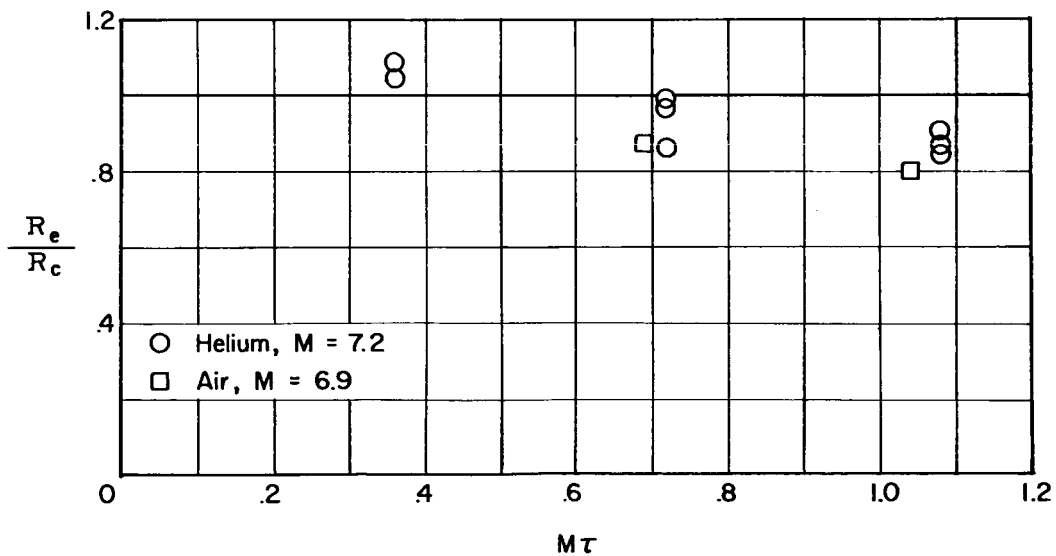
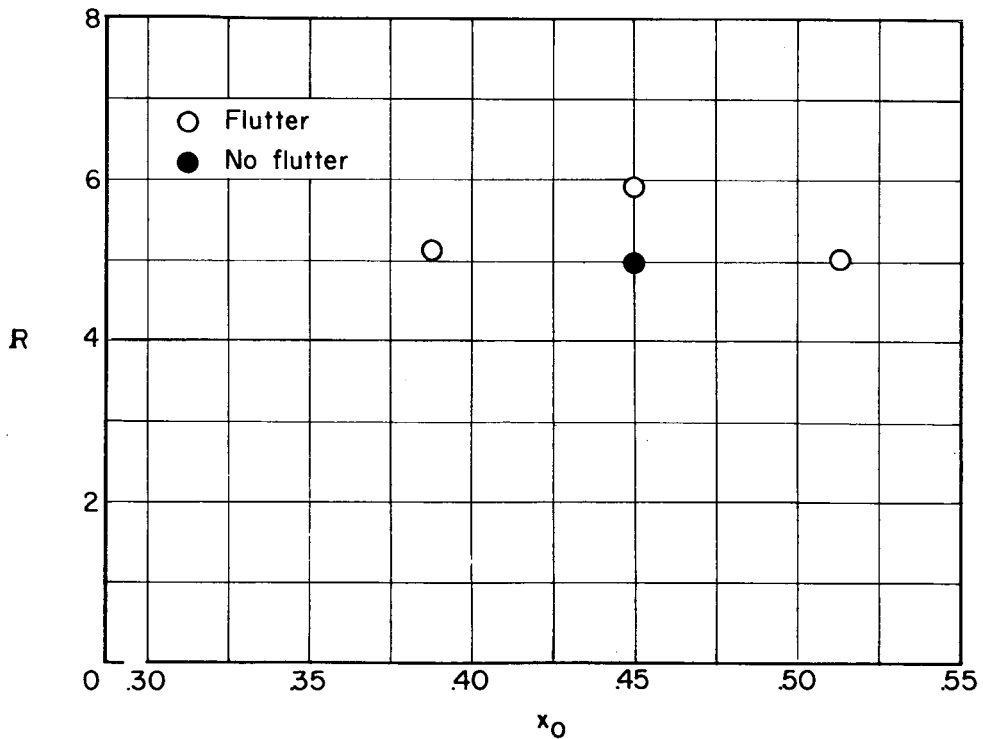(b) Ratio of experimental stiffness-altitude parameter to calculated stiffness-altitude parameter.

Figure 8.- Comparison of experimental and calculated flutter results for double-wedge models at various values of the thickness parameter $M\tau$.

$$0.31 \leqq \omega_h/\omega_\alpha \leqq 0.34; \quad x_o = 0.45; \quad R = \frac{b\omega_\alpha}{a}\sqrt{\mu}.$$

L-199

$$\frac{\omega_f}{\omega_a}$$

(a) Ratio of flutter frequency to torsional frequency.
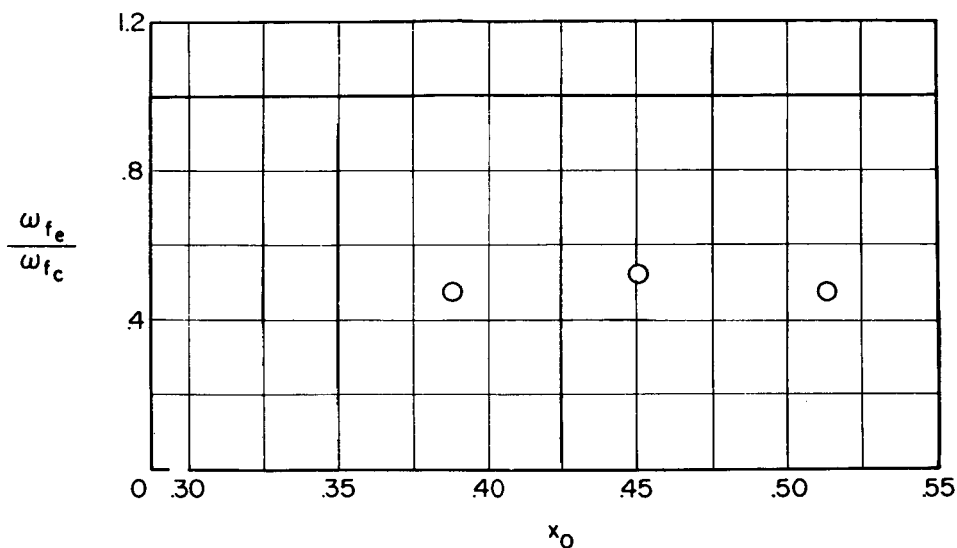
R

○ Flutter
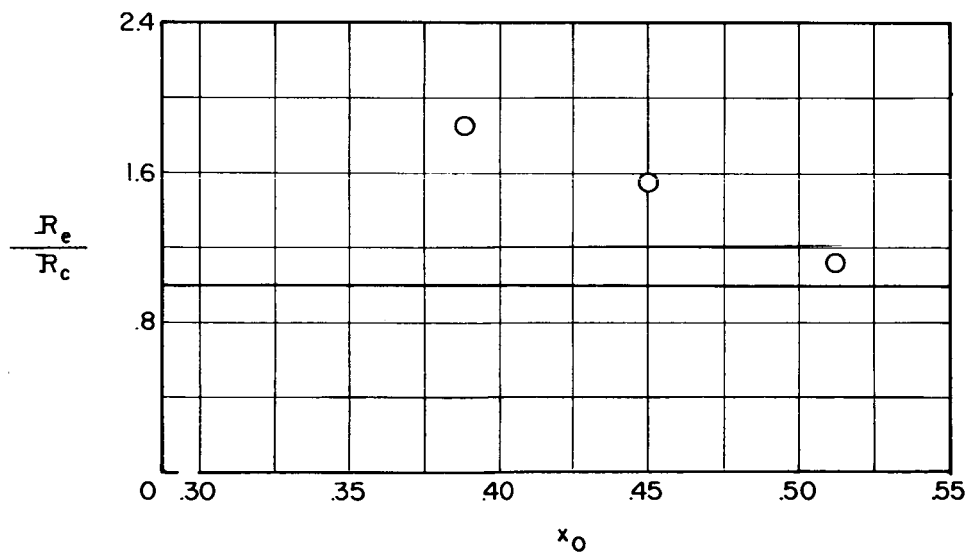● No flutter

(b) Stiffness-altitude parameter.

Figure 9.- Experimental flutter results for flat-plate models plotted against elastic-axis location. ω_h/ω_α = 0.33 and 0.34; M = 7.2 in helium; $R = \frac{b\omega_\alpha}{a}\sqrt{\mu}$.

DECLASSIFIED

(a) Ratio of experimental flutter frequency to calculated flutter frequency.

(b) Ratio of experimental stiffness-altitude parameter to calculated stiffness-altitude parameter.

Figure 10.- Comparison of experimental and calculated flutter results for flat-plate wings at various elastic-axis locations. $\omega_h/\omega_\alpha = 0.33$ and 0.34; $R = \dfrac{b\omega_\alpha}{a}\sqrt{\mu}$.

CONFIDENTIAL